Passage of a Gas Bubble through a Liquid−Liquid Interface

ARTICLE *in* INDUSTRIAL & ENGINEERING CHEMISTRY RESEARCH · SEPTEMBER 2007

Impact Factor: 2.59 · DOI: 10.1021/ie061549v

Passage of a Gas Bubble through a Liquid−Liquid Interface

Mohammed Kemiha,[†] Eric Olmos,[†] Weiyang Fei,[‡] Souhila Poncin,[†] and Huai Z. Li*[,†]

Chemical Engineering Science Laboratory (CNRS, UPR 6811), ENSIC-INPL, 1 Rue Grandville, BP 20451, 54001 Nancy cedex, France, and State Key Laboratory of Chemical Engineering, Tsinghua University, Beijing 100084, People's Republic of China

The present study aims at investigating the passage of a gas bubble at a plan liquid−liquid interface both experimentally by using a high-speed video camera and numerically through the volume-of-fluid (VOF) approach. A Newtonian silicone oil was used for the light phase while two different liquids, a Newtonian Emkarox (HV45) solution and a non-Newtonian poly(acryl amide) (PAAm) solution, were employed as the heavy phase. The passage of a gas bubble, generated from a submerged orifice, was followed during its rise in each liquid phase and in particular at the liquid−liquid interface. The original curve of the bubble's position vs time gave interesting insight into the dynamic behavior of the interface. Experimental results show the effect of the bubble size as well as the rheological properties of the heavy phase on the bubble's retention time at the liquid−liquid interface. The preliminary numerical results obtained by the VOF approach are in qualitative agreement with the experimental data.

I. Introduction

Many industrial contacting devices for mixing and separation involve two or more immiscible fluids in which discrete fluid bodies may collide with, coalesce with, or separated from one another and for which it is important to study the relative motion of fluid particles and fluid−fluid interfaces. Many contributions were made to the understanding of the breakup and coalescence mechanism. In particular, within the framework of an emulsification process, the turbulent interfacial instability, such as Rayleigh−Taylor or Kelvin−Helmholtz, between two liquid phases is usually induced by a high-shear device to produce a dispersion of oil droplets in the aqueous phase. To our best knowledge, the relationship between the droplets' size of an emulsion and the intensity of these instabilities remain still unclear.

While a great deal of research has been focused on understanding the behavior and characteristics of bubbles in both Newtonian fluids[1−3] and non-Newtonian fluids,[4−7] there have been still few experimental studies on the bubble crossing the interface between heavy and light immiscible fluids. The study of a rising bubble through a liquid−liquid interface generally concerns the evolution of the velocity and the shape of the bubble in both phases and also the behavior of the interface before and after the passage of the bubble. Lin and Slattery[8] developed a simple hydrodynamic theory for the drainage of a liquid film as a small drop or bubble approaches a fluid−fluid interface; however, they ignored the effects of London−van der Waals forces and electrostatic forces. Later, Chen et al.[9] extended this theory to include the effects of these forces. Bhaga and Weber[10] considered the fluid displacement associated with bubbles rising along the axis of a cylindrical tube. Bataille et al.[11] examined air bubbles of effective diameters 2.5−5.5 mm rising through an interface between two aqueous solutions at Reynolds numbers ranging from 500 to 1300, but they did not provide more description of the shape, the wake, and the motion of the bubble. In a similar way, Bush and Eames[12] investigated the fluid displacement associated with the translation of high Reynolds number bubbles in a thin gap and compared with a theoretical model based on a two-dimensional inviscid flow calculation. Manga and Stone[13] studied the low-Reynolds-number buoyancy-driven transition of a deformable drop toward and through a fluid−fluid interface using boundary integral method calculations. From experimental measurements, they noted that the bubble entering a less viscous fluid is extended and may break into smaller bubbles. Mohamed-Kassim and Longmire[14] examined the coalescence of single drops through planar liquid−liquid interfaces using the particle image velocimetry (PIV) device. They studied the viscosity effects at similar densities and for different Reynolds numbers varied from 10 to 26. More recently, the capillary forces acting on the spherical particles trapped at a liquid−liquid interface due to gravity-induced deformation and the mobility of charged microparticles at an oil−water interface were, respectively, investigated by Vessileva et al.[15] and Tarimala et al.[16]

The volume-of-fluid (VOF) simulation[17] is a numerical approach that describes the transient behavior of a dispersed deformable phase in another continuous phase. Its efficiency was proved for the calculation of gas dispersed flow properties such as air bubble terminal velocities and shapes in stagnant water.[18−20] For a precise prediction of ellipsoidal bubble properties, three-dimensional systems with sufficient small-grid scales have to be considered because bubble wakes exhibit three-dimensional characteristics.[21] Small spherical bubbles, whose wake is two-dimensional, are correctly simulated by axisymmetric models. These results are confirmed by Essemiani et al.[22] in the case of spherical caps. More recent studies[23] predict the influence of bubble diameter and gas holdup on the terminal velocity with a VOF approach. As far as we are concerned, VOF has never been tested for the prediction of properties of bubbles crossing a liquid−liquid interface.

The main aim is to gain insight into the fundamental mechanism of the generation of a new liquid−liquid interface as encountered in numerous industrial applications such as the emulsification process. Within an industrial piece of equipment like an Ultra-Turrax dispersor, the breakup and coalescence

* To whom correspondence should be addressed. Phone: +33 383 175 109. Fax: +33 383 322 975. E-mail: Huai-Zhi.Li@ensic.inpl-nancy.fr.

[†] ENSIC-INPL.

[‡] Tsinghua University.

10.1021/ie061549v CCC: $37.00
Published on Web 06/13/2007

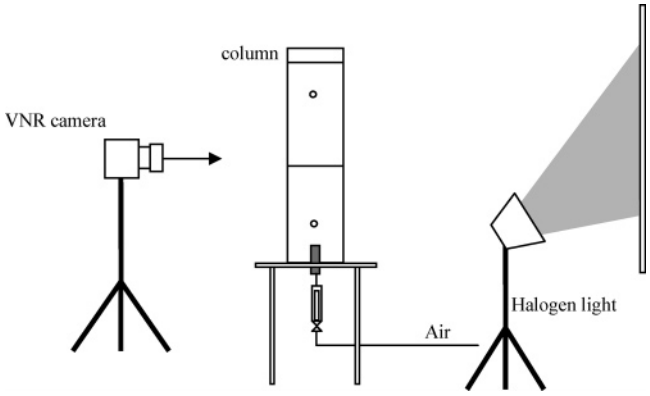

Figure 1. Experimental setup.

between droplets are so fast and occur in opaque media so that a comprehensive study is virtually impossible to date. The present work investigates experimentally with a high-speed camera as well as numerically by the VOF approach, the bubble passage at a liquid−liquid interface using as the heavy phase both Newtonian and non-Newtonian liquids. An initial plan liquid−liquid interface facilitates then the experimental observation; moreover, the size of bubbles to deform this interface is easily controllable to display different deformation dynamics of the interface.

II. Experimental Section

In this study, the experiments were conducted in a square-glass bubble column (inner dimensions: 12 cm width, 50 cm high). Bubbles were generated through a submerged orifice of 2×10^{-3} m diameter located at the center of the bottom section of the column (Figure 1). A buffer tank of 10^{-3} m^3 was placed just below the orifice and the valve to avoid fluctuations of the gas flow. An electronic valve of rapid response controlled by a personal computer permitted the injection of bubbles of determined volume at desired injection interval. In these experiments, air bubbles were always generated individually. All experiments were carried out at a constant temperature of 293 K.

Table 1. Physical Properties of Different Liquids Used in This Study

fluid	viscosity (Pa·s)	density (kg·m^{-3})	surface tension × 10^3 (N·m^{-1})
silicone oil	100×10^{-3}	965	20.2
Emkarox 65% (wt)	625×10^{-3}	1052	38.7
PAAm 0.5% (wt)	non-Newtonian	1020	72.2

In this work, two different liquids that behave as Newtonian or non-Newtonian have been considered as the heavy phase. The Newtonian liquid was a viscous lubricant Emkarox HV45 (Uniqema) dilute solution 0.65% (wt) in demineralized water. The non-Newtonian liquid was a polymeric solution of 0.5% (wt) poly(acryl amide) (PAAm AN905, SNF Floerger) in demineralized water. A Rheometrics Fluid spectrometer RFS II (Rheometric Scientific) was employed to measure the rheological properties of the non-Newtonian liquid. This revealed a shear-thinning behavior of the fluids and could be fitted by the power law model for the shear rate ranged from 0.1 to 100 s^{-1}:

$$\tau = 2.62\dot{\gamma}^{0.28} \tag{1}$$

In all experiments, a Newtonian silicone oil having a viscosity of 100×10^{-3} Pa·s (Rhodorsil 47 V 100) was used as the light phase. The surface and interfacial tensions of the solutions were measured using a Tracker tensiometer (I.T. Concept, France). The interfacial tensions between silicone oil and both Emharox 65% and PAAm 0.5% solutions were, respectively, 14.2×10^{-3} and 40.7×10^{-3} N m^{-1}. Table 1 lists additional properties of the various liquids used.

The visualization of the phenomenon was realized using a high-speed digital video system (VNR 950, Sysma Industrie) at a rate of 950 images per second, for record gray-valued images with a size of 256 × 256 pixels. The light was provided by a halogen light of 800 W, which enlightened the column via indirect lighting on a white screen behind the bubble column. The image sequences obtained were then analyzed.

III. Experimental Results

When a bubble rises in a liquid and eventually through a liquid−liquid interface, the resulting behavior can be quite

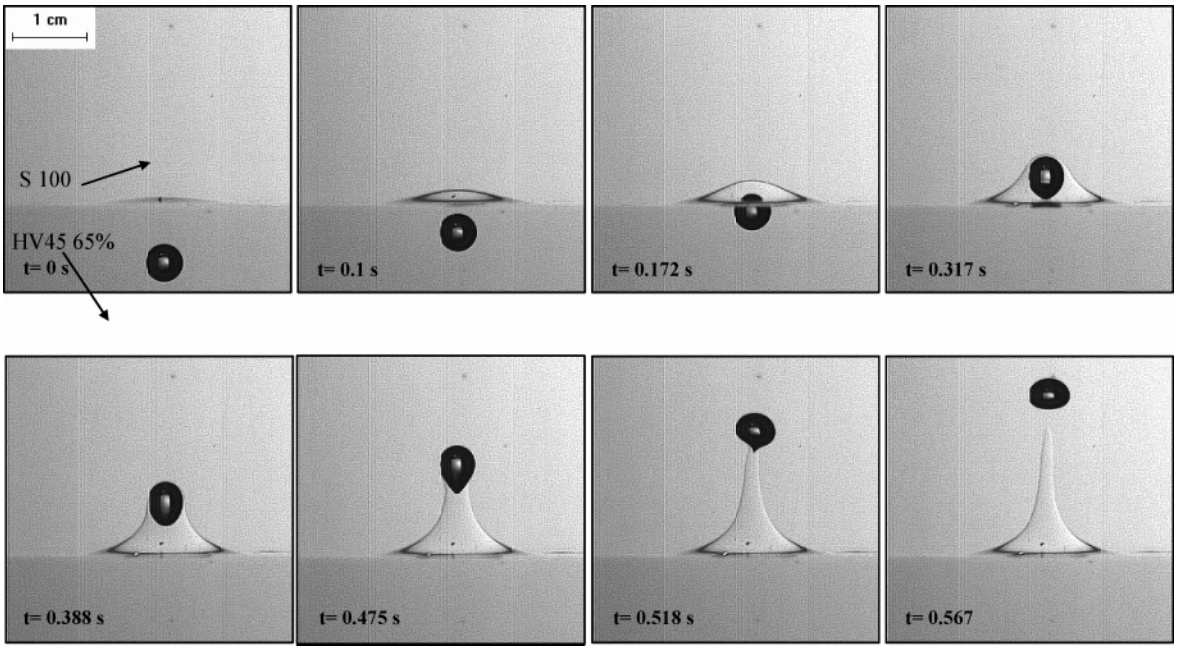

Figure 2. Passage of bubbles (d = 5.1 mm) through the Emkarox 65%−Silicone 100 interface.

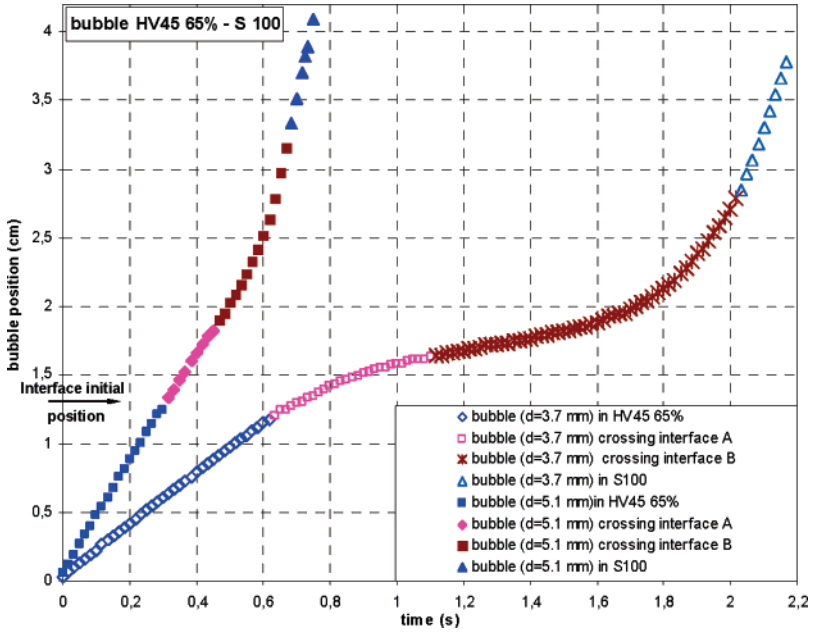

Figure 3. Bubble positions during the rise through the Emkarox 65%−Silicone 100 interface: bubble crossing interface A, the bubble front is located between the initial and the actual deformed positions of the L−L interface; bubble crossing interface B, the bubble front touches the deformed liquid−liquid interface.

different. The reduced density difference and the enhanced viscous shearing between both liquids tends to limit the bubble impact velocity in gravity-driven flow. Furthermore, the interfacial force is added to the buoyancy and viscous forces. As a result, the bubble and the interface deform significantly. The layer of the heavy surrounding liquid between the bubble and the liquid−liquid interface, termed "thin film", prevents the bubble from reaching the light phase instantaneously. In contrary to significant viscous forces, the pressure gradient within the thin film acts to drain the thin film. Eventually, the film becomes sufficiently thin so that molecular forces begin to play a main role before the rupture of the film. During the approach toward the interface, the bubble entrains a column of the heavy liquid through the interface. The rupture between this column of the heavy liquid and the bubble occurs later than the first rupture of the thin film (between the bubble front and the interface). Finally, the bubble continues its rise in the light phase.

The experimental results will first be presented for the HV45 65% as the heavy phase and Silicone 100 (S100) as the light phase, using two different sizes of bubble (with equivalent diameters of 3.7 and 5.1 mm).

Figure 2 shows the corresponding image sequences obtained by the high-speed camera. The bubble of 5.1 mm diameter has first a spherical shape under the interface and rises slowly (terminal velocity of about 0.041 m s^{-1}), then as it crosses the liquid−liquid interface it slows down and is elongated and takes a drop shape to finally achieve an oblate shape after the film rupture in the less viscous light phase with a higher terminal rise velocity of about 0.114 m s^{-1}.

Figure 3 compares the displacement of two bubbles of 3.7 and 5.1 mm equivalent diameters through the liquid−liquid interface as a function of time, with the heavy phase being the viscous Emkarox 65 wt % Newtonian solution. As expected, the higher the bubble diameter, the less was the time spent at the liquid−liquid interface, which is due to the decrease of the interfacial resistance as the bubble diameter and, therefore, the inertial forces increase.

In the case of the 0.5 wt % PAAm viscoelastic non-Newtonian heavy phase (Figure 4), the bubble has first a teardrop shape in the heavy phase due to the shear-thinning character of the polymeric solution;[24] the bubble shape does not significantly change when the bubble crosses the liquid−liquid interface and finally becomes oblate, as observed in the first case (Figure 2), with the light phase being the same.

The position of the bubble as a function of time is shown on Figure 5 for two different equivalent diameters of bubbles (d = 5.1 mm and 9.65 mm). As in the case of Newtonian heavy and light liquid−liquid interfaces, the time spent at the interface increases for decreasing bubble size. Furthermore, the comparison between Figures 3 and 5 for the same bubbles of 5.1 equiv diameter shows the contribution of the viscoelastic and shear-thinning behaviors of the heavy phase (which are added to the interfacial resistance) to the increase of the time spent at the liquid−liquid interface.

IV. Numerical Aspects

IV.1. Numerical Model. The VOF approach is used to simulate the interface crossing. It is based on the Navier−Stokes equations, which are written for the mixture phase:

$$\left\{\begin{array}{l}\dfrac{\partial \rho}{\partial t} + \nabla\cdot(\rho\mathbf{u}) = 0 \\ \dfrac{\partial(\rho\mathbf{u})}{\partial t} + \nabla\cdot(\rho\mathbf{u}\mathbf{u}) = -\nabla p - \nabla\tau + \rho\mathbf{g} + \mathbf{F_{ST}}\end{array}\right\} \quad (\text{for } i, j = l_1, l_2, g) \quad (2)$$

where l_1, l_2, and g, respectively, denote the two liquid phases and the gas phase. τ is the viscous stress tensor, and g is gravity. For a three-phase system, the density and the viscosity of the mixture phase are calculated as follows:

$$\left\{\begin{array}{ll}\rho = \sum_i \alpha_i \rho_i & (\text{for } i = l_1, l_2, g) \\ \mu = \sum_i \alpha_i \mu_i & (\text{for } i = l_1, l_2, g)\end{array}\right\} \quad (3)$$

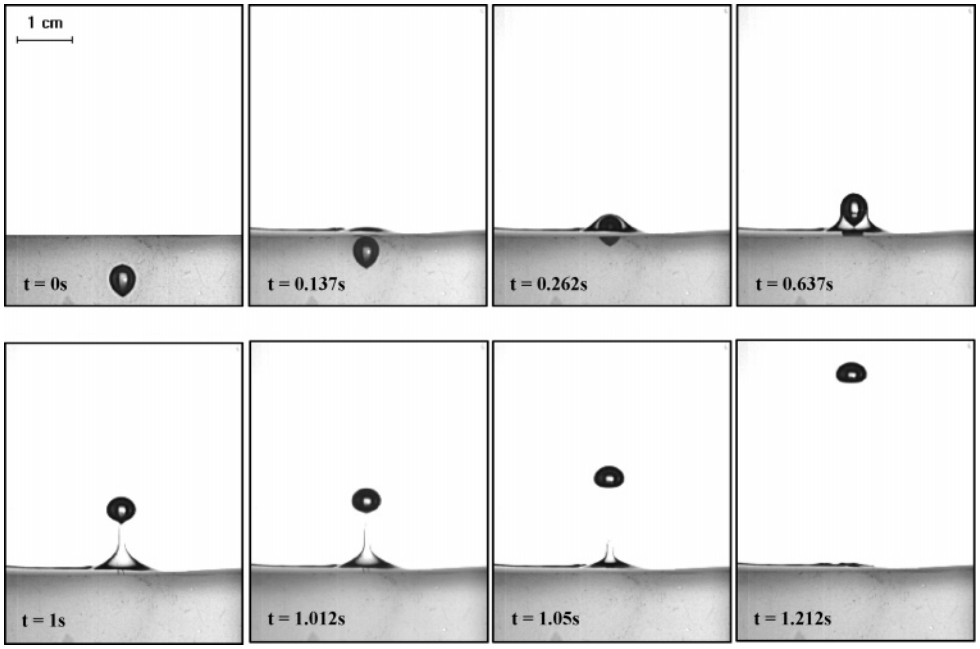

Figure 4. Images of the passage of the bubble (d = 5.1 mm) through the PAAm 0.5%−Silicone 100 interface.

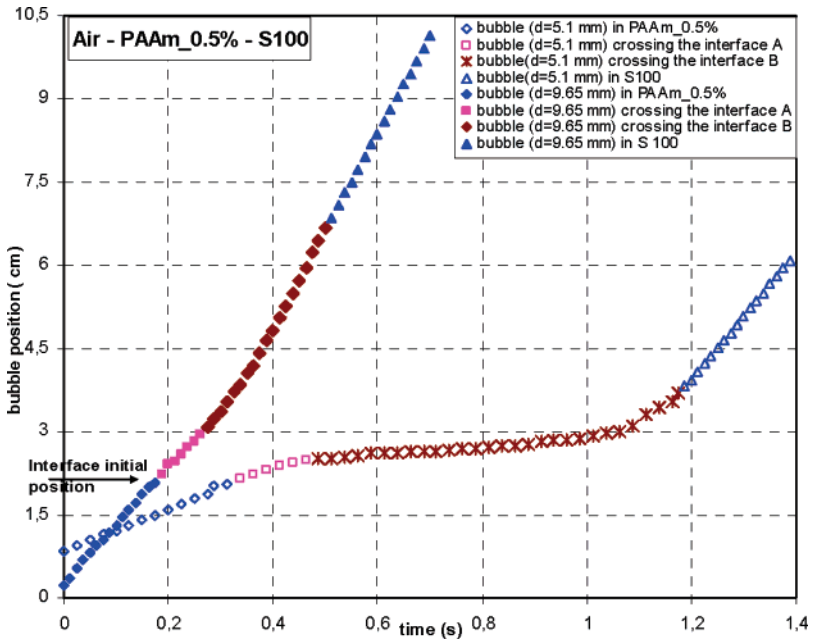

Figure 5. Bubble positions during the rise through the PAAm 0.5%−Silicone 100 interface: bubble crossing interface A, the bubble front is between the initial and the actual deformed positions of the L−L interface; bubble crossing interface B, the bubble front is in contact with the deformed L−L interface.

where $\rho_i\mu_i$ are the density and the viscosity of the pure phase. α_i is the volume fraction of phase i. In each calculation cell, the relation $\sum_i \alpha_i = 1$ is, thus, verified. The surface tension force, $\mathbf{F}_{ST}$, is obtained by Brackbill et al.:[25]

$$\mathbf{F}_{ST} = \sum_{i<j} \sigma_{ij} \frac{\alpha_i \rho_i \kappa_j \nabla a_j + \alpha_j \rho_j \kappa_i \nabla a_i}{\frac{1}{2}(\rho_i + \rho_j)} \tag{4}$$

σ_{ij} is the surface tension coefficient between phase i and phase j, and κ is the curvature.

The commercial CFD software FLUENT 6.1 is used to solve these equations numerically. Laminar flow and axisymmetry are supposed, and the interface is reconstructed by a donor−acceptor scheme. Pressure−velocity coupling is solved by a PISO algorithm, which is recommended for transient calculations. Pressure and momentum are, respectively, discretized by a PRESTO and a first-order UPWIND scheme. A constant time step of 5 ms is chosen as it offers the best compromise between calculation time and precision of the results. The domain (1 cm × 10 cm) is discretized into 12 000 cells. Calculations are performed on an AMD XP 2000+ processor; a typical calculation time is, then, approximately 2 h.

IV.2. Numerical Results. First, bubble shape and interface crossing obtained by numerical simulations are compared with our experimental results. The VOF approach clearly appears as a powerful tool for predicting qualitatively the crossing of a liquid−liquid interface by an air bubble. Typical results of interface deformation are shown in Figure 6 in the case of the Newtonian Emkarox 65%−Silicone 100. The major phenomena encountered are well-represented: bubble rise in the heavier

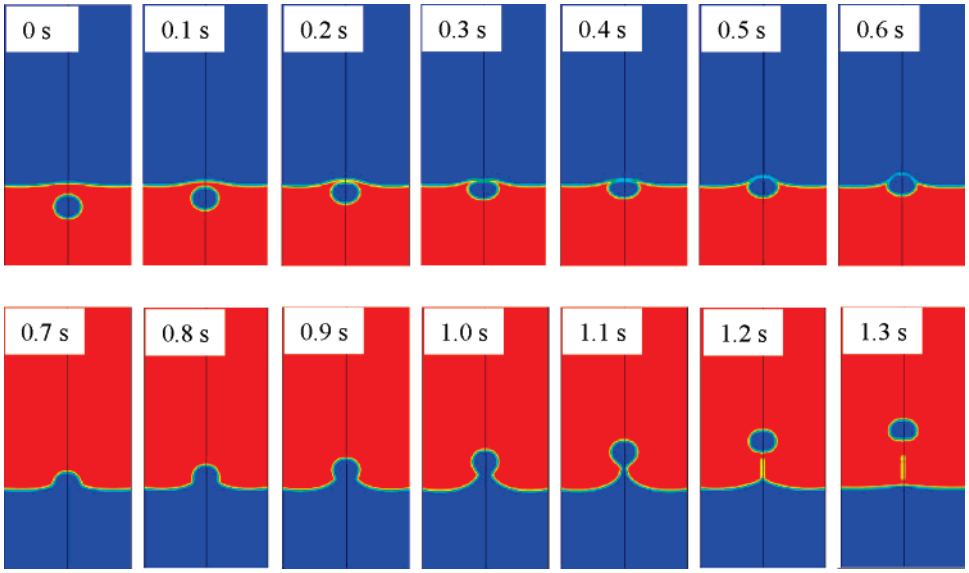

Figure 6. Typical results of VOF simulations: system, HV45 65%−Silicone 100; time step between each picture, 0.1 s. Colors of the heavy phase and of the light phase are inverted when the bubble reaches the interface (top and bottom figures).

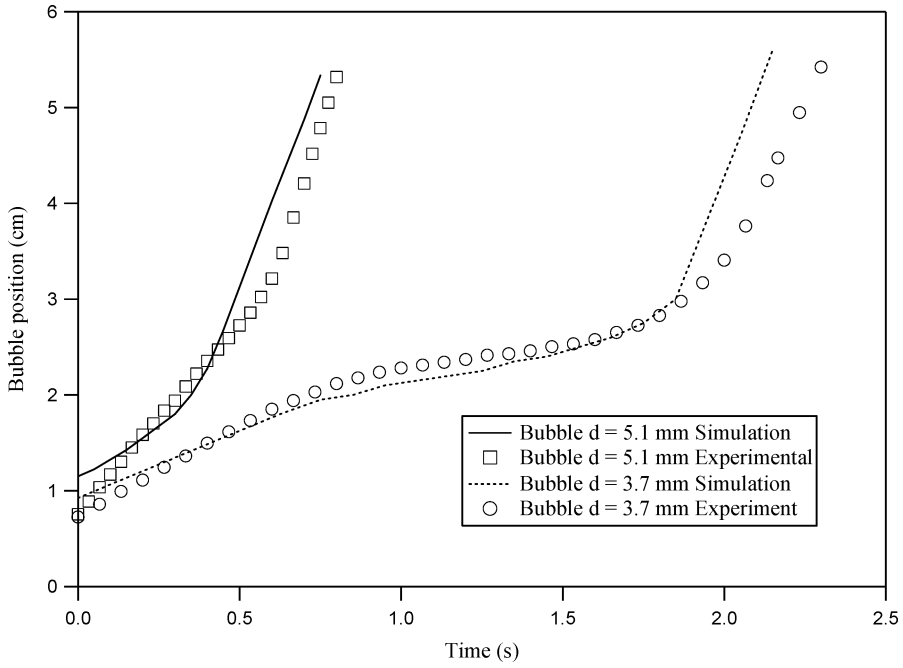

Figure 7. Computed bubble (d = 3.7 mm and d = 5.1 mm) positions during the rise through the HV45 65%−Silicone 100 interface and comparison with experiments.

Table 2. Results Obtained by Both the Experiments and Numerical Simulation

system	HV45 65%−S100			PAAm 0.5%−S100	
bubble diameter (mm)	3.7 experimental	5.1 experimental	3.7 numerical	5.1 experimental	9.65 experimental
bubble rise velocity in the heavier phase ($cm \cdot s^{-1}$)	1.86	4.1	1.4	3.85	10.64
time spent by the bubble at the liquid−liquid interface (s)	1.41	0.33	1.2	0.77	0.17
bubble rise velocity in the lighter phase ($cm \cdot s^{-1}$)	7.0	11.4	8.7	11.44	17.38

phase, interface deformation with bubble slowdown, gas−liquid film rupture, and heavier phase trapping in the lighter phase.

Second, the bubble velocities are quantitatively studied (see Figure 7). These results show that the change in bubble-rise velocity when crossing the liquid−liquid interface is clearly predicted. Furthermore, bubble stagnation at the liquid−liquid interface is well put into evidence, too. Quantitatively, it can be noticed that, as expected, the VOF approach only gives a correct approximation of bubble velocities in the heavy phase: 1.4 $cm \cdot s^{-1}$ (see Table 2). In the light phase, this estimation is more precise (8.7 $cm \cdot s^{-1}$). For these fluids, viscous forces are indeed predominant and, therefore, lead to stabilized two-dimensional bubble wakes, which are better simulated by axisymmetric models. Last, it can be seen that the time needed by the bubble to cross the interface is largely underestimated. This is due to the fact that the simulation of the liquid film

draining and rupture is not precise enough. The surface tension model is probably not sufficient when considering these very small scales. Moreover, a correct modeling of these phenomena should include dramatically small grid sizes (submicrometer) and local interface curvature.

Future work will be based on three-dimensional systems and on the use of non-Newtonian fluids. The use of particle image velocimetry will furthermore allow the comparison of the liquid velocity fields.

V. Conclusion

Experimental and numerical results of the flow of a single bubble across a liquid−liquid interface have been presented. While the light phase was always a viscous Newtonian solution, both Newtonian and non-Newtonian solutions were considered as the heavy phase. Two different bubble sizes have been used in order to compare the effect of the bubble size on the time spent at the liquid−liquid interface. Experimental results show the logical increase of the time spent at the liquid−liquid interface with the decrease of the bubble's diameter for both the Newtonian and the non-Newtonian heavy phases due to the interfacial resistance and also the effect of the viscoelastic aspects and the shear-thinning behavior of the heavy phase on the increase of this retention time.

A qualitative agreement between experimental and numerical results was obtained for the bubble position versus time and the bubble velocities of bubbles crossing a Newtonian heavy liquid and a Newtonian light liquid interface. Further investigation on the temporary shape evolution of the thin film could lead to a better understanding of the coalescence mechanism as well as the VOF modeling.

Acknowledgment

One of the authors, W.F., wishes to thank the Grant sponsor No. 2001CB711203 of the Key Program for International Cooperation of Science and Technology, China.

Nomenclature

d = equivalent bubble diameter (m)
$\mathbf{F}_{ST}$ = surface tension force
g = gravitational acceleration ($m \cdot s^{-2}$)
K = consistency ($Pa \cdot s^n$)
n = flow index
Re = Reynolds number
U = terminal rise velocity ($m \cdot s^{-1}$)

Greek Letters

α_i = volume fraction of phase i
$\dot{\gamma}$ = shear rate (s^{-1})
σ = surface tension ($N \cdot m^{-1}$)
κ = curvature (m)
μ = viscosity (Pa·s)
ρ = fluid density ($kg \cdot m^{-3}$)
τ = stress (Pa)

Literature Cited

(1) Clift, R.; Grace, F. J.; Weber, M. E. *Bubbles, drops and particles*; Academic Press: New York, 1978.

(2) Jamialahmadi, M.; Branch, C.; Müller-Steinhagen, H. Terminal bubble rise velocity in liquids. *Trans. Inst. Chem. Eng.* **1994**, *72*, 119−122.

(3) Frank, X.; Funfschilling, D.; Midoux, N.; Li, H. Z. Bubbles in a viscous liquid: Lattice Boltzmann simulation and experimental validation. *J. Fluid Mech.* **2006**, *546*, 113−122.

(4) Chhabra, R. P. *Bubbles, Drops and Particles in Non-Newtonian Fluids*; CRC Press: Boca Raton, FL, 1993.

(5) Funfschilling, D.; Li, H. Z. Flow of non-Newtonian fluids around bubbles: PIV measurements and birefringence visualization. *Chem. Eng. Sci.* **2001**, *56*, 1137−1141.

(6) De Kee, D.; Chan Man Fong, C. F. Bubble shape in non-Newtonian fluids. *J. Appl. Mech.* **2002**, *69*, 703−704.

(7) Frank, X.; Li, H. Z. Complex flow around a bubble rising in a non-Newtonian fluid. *Phys. Rev. E* **2005**, *71*, 036309.

(8) Lin, C. Y.; Slattery, J. C. Thinning of a liquid film as a small drop or bubble approaches a fluid−fluid interface. *AIChE J.* **1982**, *28*, 792−798.

(9) Chen, J. D.; Hahn, P. S.; Slattery, J. C. Coalescence time for a small drop or bubble at a fluid−fluid interface. *AIChE J.* **1984**, *30*, 622−630.

(10) Bhaga, D.; Weber, M. E. Bubbles in viscous liquids: Shapes, wakes and velocities. *J. Fluid Mech.* **1981**, *105*, 61−85.

(11) Bataille, J.; Lance, M.; Marie, J. L. In *Phase-Interface Phenomena in Multiphase Flow*; Hewitt, G. F., Mayinger, F., Riznic, J. R., Eds.; Hemisphere Publishing Corp.: New York, 1991; p 179.

(12) Bush, J. W. M.; Eames, I. Fluid displacement by high Reynolds number bubble motion in a thin gap. *Int. J. Multiphase Flow* **1998**, *24*, 411−430.

(13) Manga, M.; Stone, H. A. Low Reynolds number motion of bubbles, drops and rigid spheres trough fluid−fluid interfaces. *J. Fluid Mech.* **1995**, *287*, 279−298.

(14) Mohamed-Kassim, Z.; Longmire, E. K. Drop coalescence through a liquid/liquid interface. *Phys. Fluids* **2004**, *16*, 2170−2181.

(15) Vessileva, N. D.; van den Ende, D.; Mugele, F.; Mellema, J. Capillary forces between spherical particles floating at a liquid−liquid interface. *Langmuir* **2005**, *21*, 11190−11200.

(16) Tarimala, S.; Ranabothu, S. R.; Vernetti, J. P.; Dai, L. L. Mobility and in situ aggregation of charged microparticles at oil−water interfaces. *Langmuir* **2004**, *20*, 5171−5173.

(17) Hirt, C.; Nichols, B. Volume of fluid (VOF) method for the dynamics of free boundaries. *J. Comput. Phys.* **1981**, *39*, 201−225.

(18) Delnoij, E.; Kuipers, J.; van Swaaij, W. P. M. Computational Fluid Dynamics Applied to Gas−Liquid Contactors. *Chem. Eng. Sci.* **1997**, *52*, 3623−3638.

(19) Rudman, M. Volume-tracking methods for interfacial flow calculations. *Int. J. Numer. Methods Fluids* **1997**, *24*, 671−691.

(20) Krishna, R.; van Baten, J. Simulating the motion of gas bubbles in a liquid. *Nature* **1999**, *398*, 208.

(21) Olmos, E. Etude expérimentale et numérique des écoulements gaz-liquide en colonnes à bulles, Ph.D. Thesis, INPL, Nancy, France, 2002.

(22) Essemiani, K.; Ducom, G.; Cabassud, C.; Line, A. Spherical cap bubbles in a flat sheet nanofiltration module: Experiments and numerical simulation. *Chem. Eng. Sci.* **2001**, *56*, 6321−6327.

(23) Bertola, F.; Grundseth, J.; Hagesaether, L.; Dorao, C.; Luo, H.; Hjarbo, K. W.; Svendsen, H. F.; Vanni, M.; Baldi, G.; Jakobsen, H. A. Numerical analysis and experimental validation of bubble size distributions in two-phase bubble column reactors. *Multiphase Sci. Technol.* **2005**, *17*, 123−145.

(24) Frank, X.; Li, H. Z.; Funfschilling, D.; Burdin, F.; Ma, Y. Bubble motion in non-Newtonian fluids and suspensions. *Can. J. Chem. Eng.* **2003**, *81*, 483−490.

(25) Brackbill, J. D.; Kothe, J. D.; Zemach, C. A continuum method for modelling surface tension. *J. Comput. Phys.* **1992**, *100*, 335−354.

Received for review December 3, 2006
Revised manuscript received May 2, 2007
Accepted May 3, 2007

IE061549V